Title

Revealing the mechanism of action of a first-in-class covalent inhibitor of KRASG12C (ON) and other functional properties of oncogenic KRAS by 31P NMR.

Journal

Journal of Biological Chemistry, 300(2)

Authors

Maciag, Anna
Sharma, Alok
Pei, Jun
et al.

Publication Date

2024-02-01

DOI

10.1016/j.jbc.2024.105650

Peer reviewed

JBC COMMUNICATION

Revealing the mechanism of action of a first-in-class covalent inhibitor of KRASG12C (ON) and other functional properties of oncogenic KRAS by ^{31}P NMR

Received for publication, September 18, 2023, and in revised form, December 27, 2023 Published, Papers in Press, January 16, 2024,
https://doi.org/10.1016/j.jbc.2024.105650

Alok K. Sharma[1,*], Jun Pei[2], Yue Yang[2], Marcin Dyba[1], Brian Smith[1], Dana Rabara[1], Erik K. Larsen[1], Felice C. Lightstone[2], Dominic Esposito[1], Andrew G. Stephen[1], Bin Wang[3], Pedro J. Beltran[3], Eli Wallace[3], Dwight V. Nissley[1], Frank McCormick[1,3,4], and Anna E. Maciag[1,*]

From the [1]NCI RAS Initiative, Cancer Research Technology Program, Frederick National Laboratory for Cancer Research, Leidos Biomedical Research, Inc, Frederick, Maryland, USA; [2]Physical and Life Sciences (PLS) Directorate, Lawrence Livermore National Laboratory, Livermore, California, USA; [3]BridgeBio Oncology Therapeutics, BridgeBio Pharma, Inc, Palo Alto, California, USA; [4]Helen Diller Family Comprehensive Cancer Center, University of California San Francisco, San Francisco, California, USA

Reviewed by members of the JBC Editorial Board. Edited by Phillip A. Cole

Individual oncogenic KRAS mutants confer distinct differences in biochemical properties and signaling for reasons that are not well understood. KRAS activity is closely coupled to protein dynamics and is regulated through two interconverting conformations: state 1 (inactive, effector binding deficient) and state 2 (active, effector binding enabled). Here, we use ^{31}P NMR to delineate the differences in state 1 and state 2 populations present in WT and common KRAS oncogenic mutants (G12C, G12D, G12V, G13D, and Q61L) bound to its natural substrate GTP or a commonly used nonhydrolyzable analog GppNHp (guanosine-5'-[(β,γ)-imido] triphosphate). Our results show that GppNHp-bound proteins exhibit significant state 1 population, whereas GTP-bound KRAS is primarily (90% or more) in state 2 conformation. This observation suggests that the predominance of state 1 shown here and in other studies is related to GppNHp and is most likely nonexistent in cells. We characterize the impact of this differential conformational equilibrium of oncogenic KRAS on RAF1 kinase effector RAS-binding domain and intrinsic hydrolysis. Through a KRAS G12C drug discovery, we have identified a novel small-molecule inhibitor, BBO-8956, which is effective against both GDP- and GTP-bound KRAS G12C. We show that binding of this inhibitor significantly perturbs state 1–state 2 equilibrium and induces an inactive state 1 conformation in GTP-bound KRAS G12C. In the presence of BBO-8956, RAF1–RAS-binding domain is unable to induce a signaling competent state 2 conformation within the ternary complex, demonstrating the mechanism of action for this novel and active-conformation inhibitor.

KRAS is mutated in almost 30% of human cancers, including pancreatic, colorectal, and lung cancers, and is a major drug target in oncology (1–4). Mutations at G12, G13, and Q61 positions lead to extended GTP-bound active states of RAS that enable strong and dysregulated mitogen-activated protein kinase/extracellular signal–regulated kinase (ERK) and PI3K signaling resulting in oncogenesis (4).

The RAS G-domain (amino acids 1–169) includes several flexible regions including the P-loop (amino acids 10–17) that binds nucleotide phosphates and switch I (SW1; amino acids 25–40) and switch II (SW2; amino acids 57–75) that interact directly with effector proteins including RAF, PI3K, and RalGDS. The inherent flexibility of these regions is associated with population equilibria of at least two interconverting conformational states known as "state 1" and "state 2" when guanosine triphosphate nucleotide is bound (5–7). The active state 2 conformation binds to the RAS-binding domain (RBD) of effector proteins, whereas state 1 is inactive since binding affinity is reduced at least two orders of magnitude (8, 9). State 1–state 2 equilibrium was originally described through the NMR analysis of two γ-phosphate conformations (γ_1 and γ_2) apparent when RAS is bound to GTP and its analogs (10-12). Differences between the ^{31}P chemical shift values of free GTP nucleotide *versus* when RAS bound are described elsewhere (11). X-ray crystallography provides invaluable three-dimensional structural information of RAS proteins; however, in most crystals, the SW regions governing RAS function are not well resolved, and therefore, provide limited information on the intrinsic conformational dynamics in WT and oncogenic RAS. Solution-state ^{31}P NMR spectroscopy can capture and quantify these γ_1 and γ_2 peaks (slowly exchanging on the NMR timescale) representing state 1 and state 2 conformations, respectively, as demonstrated by the pioneering work by Kalbitzer *et al.* (11–13).

The chemical shifts of peaks in state 1–state 2 equilibrium dynamics driven by the γ-phosphate have been characterized for WT and select mutants of HRAS in complex with GppNHp (guanosine-5'-[(β,γ)-imido] triphosphate) and for WT HRAS-GTP (11–13) and other RAS family GTPases (14). Growing evidence, however, suggests that KRAS and HRAS behave differently and exhibit mutant-specific distinct conformational features (7, 15, 16). The populations of

* For correspondence: Alok K. Sharma, alok.sharma@nih.gov; Anna E. Maciag, anna.maciag@nih.gov.

conformational equilibrium of γ_1–γ_2 governing the dynamic properties of active WT KRAS and most common oncogenic mutants (G12C, G12D, G12V, Q61L, and G13D) have not been characterized and compared. Detailed characterization of these conformational states, especially for KRAS oncogenic mutants, can provide valuable insights for drug design.

RAS has long been considered a therapeutically undruggable target (17). The cysteine mutation at codon 12 (G12C) is a frequent KRAS alteration found in human cancer, and its reactivity makes it a target for therapeutic development. Recent efforts have identified a series of novel inhibitors that bind in the SW2/α3 (SIIP) pocket and covalently react with the thiol group of cysteine 12 (18–22). Clinical inhibitors AMG510 (Sotorasib) (20) and MRTX849 (Adagrasib) (21) target inactive GDP-bound KRAS G12C, whereas phase 1 inhibitor RMC-6291 targets the GTP-bound form of KRAS G12C in a cyclophilin A-dependent manner (23). We have identified a potent covalent small molecule (BBO-8956) that selectively binds to KRAS G12C in SW2/α3 pocket, in both active (GTP-bound) and inactive (GDP-bound) conformation.

Herein, using ^{31}P NMR spectroscopy, we performed a comparative analysis of the population distribution of state 1 and state 2 conformations present in WT and oncogenic mutants of KRAS bound to GTP or its nonhydrolyzable analog GppNHp. We show that these population distributions relate to the biochemical and functional properties of these proteins. We demonstrate that BBO-8956 effectively binds GTP-KRAS G12C, shifts state 1–state 2 equilibrium to an inactive "substate" representing state 1-like conformation, and disrupts the effector binding and downstream oncogenic signaling. To our knowledge, this is the first study that deciphers the molecular mechanism of a small-molecule direct inhibitor of GTP-KRAS through perturbation of state 1–state 2 equilibrium and highlights the utility of ^{31}P NMR in the drug-discovery process.

Results and discussion

Conformational equilibria of GppNHp-KRAS WT and oncogenic mutants

Figure 1*A* shows the ^{31}P NMR spectrum of WT KRAS-GppNHp that represents the conformational sampling between the two distinct states, state 1 and state 2, mainly represented by the γ_1 and γ_2 peaks, respectively. Previous X-ray crystallography studies revealed that in state 1 conformation, the SW1 region (and tyrosine 32, Y32) is generally packed away from the nucleotide in an "open" orientation (24), whereas in state 2 conformation, SW1 (and Y32) packs closer to the nucleotide in a "closed" orientation (25). The ^{31}P NMR analyses on the qualitative measurements of state 1 and state 2 conformational equilibria in the active form of WT and oncogenic KRAS are discussed below.

Figure 1*B* shows the overlay of ^{31}P spectra of WT and oncogenic mutants (G12C, G12D, G12V, Q61L, and G13D) of GppNHp-bound KRAS. Peaks corresponding to phosphorous atoms in α-, β-, and γ-phosphate groups of the nucleotide are observed. Peaks α_1, β_1, and γ_1 represent the inactive conformation (state 1), whereas α_2, β_2, and γ_2 represent the presence of an active conformation (state 2) of the protein. Chemical shift values of these peaks are summarized in Table S1. γ_1 and γ_2 peaks corresponding to the state 1 and state 2 population distribution indicate that the inactive state 1 conformation is more prevalent (Fig. 1*C*). KRAS G12V possesses the highest state 1 frequency (∼71%), whereas WT and G12C are lowest. State 1 rank-order frequency profile for codon 12 mutants in KRAS-GppNHp is G12V > G12D > G12C > WT. KRAS Q61L and G13D mutants also exhibit a predominant state 1 population. Chemical shifts of γ_1 and γ_2 peaks are not well resolved in the G13D spectrum because of their partial overlap and that could affect accurate population determination, as noted elsewhere (26). Reported binding affinities between the RAF1-RBD and WT and oncogenic mutants of KRAS-GppNHp follow the codon 12 rank order as (in decreasing order) G12V < G12D < G12C < WT, whereas Q61L and G13D proteins show higher affinities than G12V (27). These data are in close agreement with our ^{31}P NMR results showing a similar trend and suggest that higher state 1 prevalence correlates with lower RAF1-RBD binding affinity.

The T35S mutation causes active RAS to shift state 1–state 2 equilibrium toward state 1 conformation, resulting in decreased conformational freedom of P-loop, SW1, and SW2 regions (13). We confirmed the identification of γ_1 and γ_2 peaks in the aforementioned spectra using the data collected for these proteins harboring T35S mutations (Fig. 1*D*).

Conformational equilibria of GTP-bound KRAS WT and oncogenic mutants

State 1–state 2 conformational flux evident in the ^{31}P spectra for KRAS-GTP is strikingly different from that of KRAS-GppNHp (Fig. 2*A*). About 90% or more of the GTP-bound populations are state 2, and only a minor population is present in state 1 conformation (Fig. 2*B*), in congruence with data reported for HRAS-GTP (11). A qualitative analysis indicates that KRAS G12V possesses the highest state 1 population (∼11%), whereas G12C has the lowest (4%). The rank order of state 1 for codon 12 mutants in KRAS-GTP is G12V > G12D > WT > G12C (Fig. 2*B*). State 1 population for Q61L and G13D proteins is between G12D and G12V proteins. Chemical shifts of G13D γ_1 and γ_2 peaks likely exhibit a partial peak overlap and could affect accurate population determination. The chemical shift values for these peaks are summarized in Table S2*A*. Thus, WT and oncogenic mutants sample different conformational equilibrium and induce a varying degree of structural plasticity, which is most likely coupled with the SW1 and SW2 dynamics. Given this significant difference in state 1–state 2 population equilibrium for KRAS-GTP *versus* KRAS-GppNHp, it appears important to monitor the corresponding biological effects by measuring effector engagement and binding affinities of KRAS in complex with GTP, compared to those with the non-natural analog GppNHp (28).

Interestingly, quantitation of the free-phosphate peak (P_i) (Fig. 2*C*) could be a measure of intrinsic hydrolysis rate.

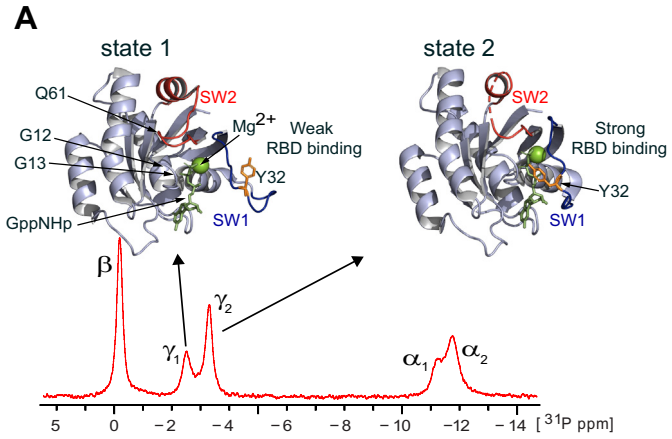

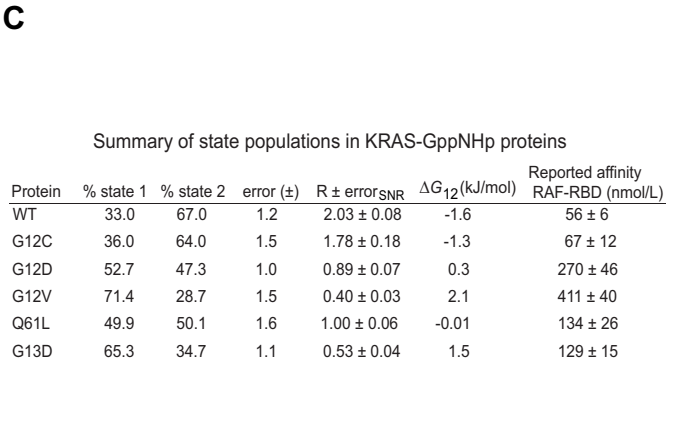

Summary of state populations in KRAS-GppNHp proteins

Protein	% state 1	% state 2	error (±)	R ± error$_{SNR}$	ΔG_{12}(kJ/mol)	Reported affinity RAF-RBD (nmol/L)
WT	33.0	67.0	1.2	2.03 ± 0.08	-1.6	56 ± 6
G12C	36.0	64.0	1.5	1.78 ± 0.18	-1.3	67 ± 12
G12D	52.7	47.3	1.0	0.89 ± 0.07	0.3	270 ± 46
G12V	71.4	28.7	1.5	0.40 ± 0.03	2.1	411 ± 40
Q61L	49.9	50.1	1.6	1.00 ± 0.06	-0.01	134 ± 26
G13D	65.3	34.7	1.1	0.53 ± 0.04	1.5	129 ± 15

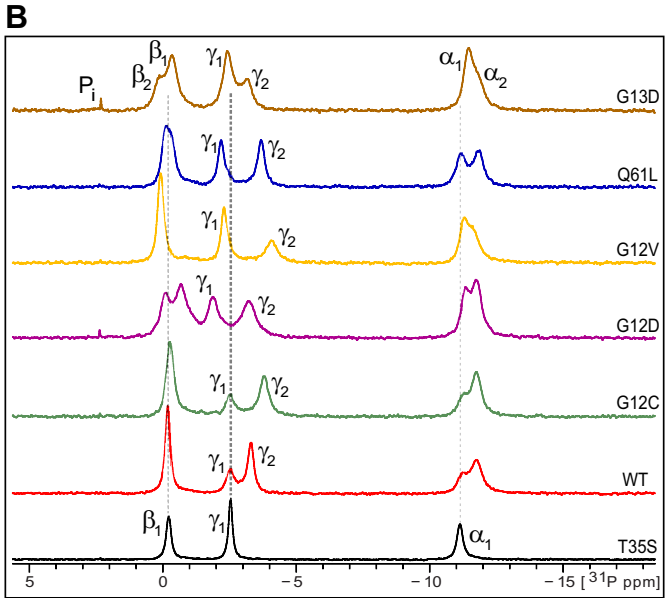

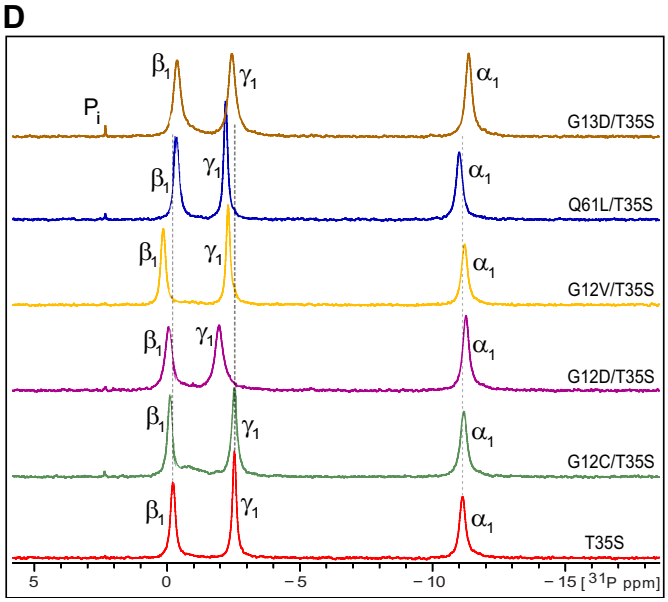

Figure 1. State 1 and state 2 conformational equilibria in KRAS-GppNHp. *A*, one-dimensional ^{31}P NMR spectrum of WT KRAS-GppNHp at 278 K. The α_1, γ_1 and α_2, γ_2 peaks represent state 1 and state 2 conformations of RAS protein, respectively. Crystal structures of state 1 (Protein Data Bank code: 4EFL) and state 2 (Protein Data Bank code: 6VC8) conformations of RAS protein are shown. Nucleotide GppNHp-binding site and the oncogenic mutation sites are highlighted. *B*, stack plot of ^{31}P NMR spectra of WT and oncogenic mutants at 278 K. At the *bottom* is shown the spectrum for T35S variant of WT protein that represents peaks belonging to state 1 conformation. *C*, qualitative measurement of state 1 and state 2 conformational populations from the absolute intensities of γ_1 and γ_2 peaks in the spectra shown in *B*. Peak intensity error and uncertainty estimation in γ_2/γ_1 peak ratio (R) were deduced as detailed in the *Supporting information* section. ΔG_{12} represents difference in free energy between state 1 and state 2. The literature reported RAF1 RBD binding affinities of WT and mutant KRAS proteins (27). *D*, stack plot of spectra harboring T35S mutation. GppNHp, guanosine-5′-[(β,γ)-imido] triphosphate; RBD, RAS-binding domain.

Decreased P_i peak intensity is noted in G12V and Q61L spectra (Fig. 2, *A* and *C*). A similar analysis makes it possible to estimate non-GAP mediated (intrinsic) hydrolysis of KRAS-GTP establishing the rank of WT > G12C > G13D > G12D > G12V > Q61L, which is consistent with the published intrinsic hydrolysis rates (except G13D) of these proteins (27, 29). This observation is congruent with the emerged peak intensity noted for the α- and β-phosphate groups of GDP because of GTP hydrolysis occurring on the NMR timescale. Significantly decreased intensities of GDP peaks seen in the spectra of G12V and Q61L proteins (Fig. 2, *A* and *C*) are consistent with their established slower intrinsic hydrolysis rates. Identification of γ_1 and γ_2 peaks in Figure 2*A* were confirmed by comparison to data from T35S KRAS-GTP proteins (Fig. 2*D* and Table S2*B*).

To avoid GTP stability issues, most work in structural biology, biophysics, and biochemistry of RAS uses the non-hydrolyzable GTP analog GppNHp. Our results indicate that GppNHp binding alters the conformational flux in favor of state 1 conformation, presumably because of rearrangement of interactions between the SW regions and the nucleotide. In contrast, GTP-bound oncogenic KRAS has state 2 as the dominant conformation (Figs. 1*B*, 2*A*, and S3*D*). Notably, the crystal structures of WT and various RAS mutants including G12V (Protein Data Bank [PDB] code: 4EFM), Q61L (PDB code: 4EFN), and G13D bound to GppNHp (PDB codes: 6E6C and 6E6P) or bound to GMPPCP frequently adopt state 1 conformation (24, 30, 31). In such a scenario, the SW regions likely require less entropic contribution to achieve the lower energy, stable, and "open" state 1 conformer, and this is

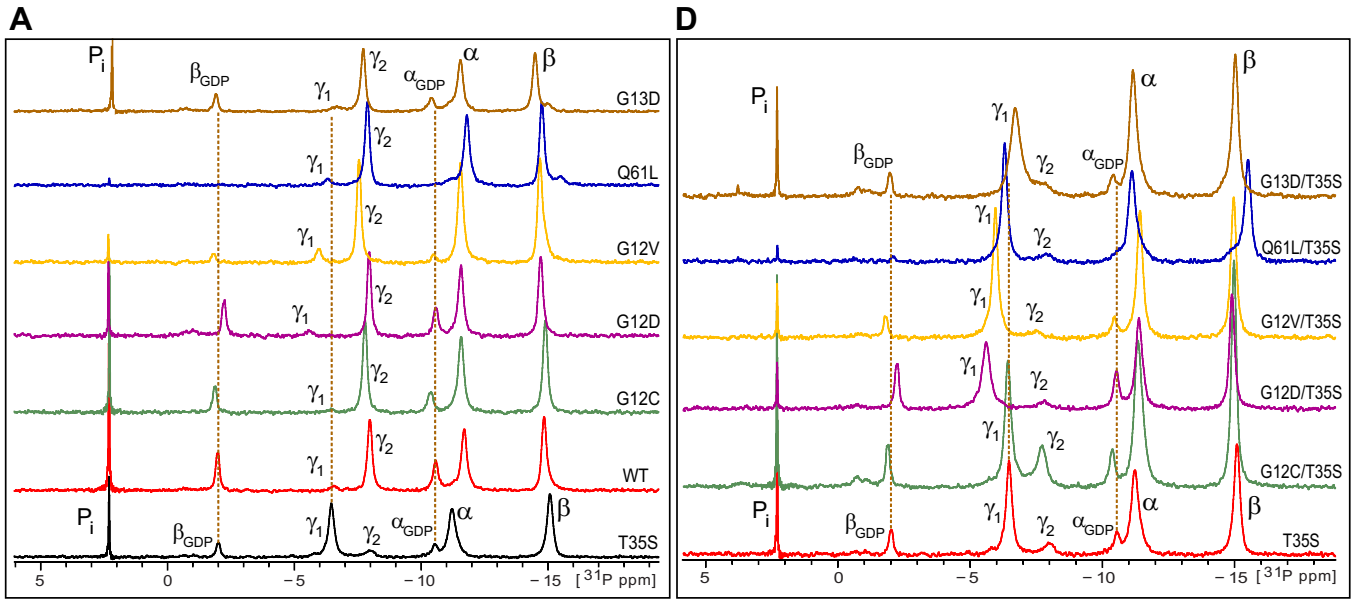

B

Summary of state populations in KRAS-GTP proteins

Protein	% state 1	% state 2	error (±)	R	ΔG_{12}(kJ/mol)	state 1/state 2 ± SEM MD Sim
WT	6.1	93.9	1.9	15.39	-6.3	3.1/96.9 ± 0.4
G12C	3.9	96.1	1.7	24.64	-7.4	4.6/95.4 ± 1.4
G12D	6.3	93.7	2.1	14.87	-6.2	8.7/91.3 ± 1.4
G12V	11.5	88.5	1.5	7.70	-4.7	18.1/81.9 ± 2.5
Q61L	7.3	92.7	1.7	12.70	-5.9	8.7/91.3 ± 0.4
G13D	7.7	92.3	1.3	11.99	-5.7	6.9/93.1 ± 0.7

C

Summary of free phsphate peak intensity and extent of intrinsic hydrolysis in KRAS-GTP proteins

Protein	P_i	error (±)	R ± $error_{SNR}$	Reported rate of hydrolysis Intrinsic GTP (10^{-5} s^{-1})
WT	74.0	0.4	2.85 ± 0.07	68 ± 3.5
G12C	43.3	0.5	1.67 ± 0.05	49 ± 1.8
G12D	23.0	0.9	0.88 ± 0.04	19 ± 1.0
G12V	6.9	1.2	0.27 ± 0.02	4.2 ± 0.2
Q61L	2.1	1.7	0.08 ± 0.02	0.8 ± 0.05
G13D	39.0	0.4	1.50 ± 0.04	9.6 ± 0.2

Figure 2. State 1 and state 2 conformational equilibria in KRAS-GTP. *A*, stack plot of ^{31}P NMR spectra of WT and oncogenic mutants at 278 K. At the *bottom* is shown the spectrum for T35S variant of WT protein that represents peaks belonging to state 1 conformation. *B*, qualitative measurement of state 1 and state 2 conformational populations deduced from the absolute intensities of γ_1 and γ_2 peaks in the spectra shown in A. Error in peak intensity measurement and the peak ratio (R) as determined in the spectra. ΔG_{12} represents difference in free energy between state 1 and state 2 (ΔG_{12}). Molecular dynamics (MD) simulation estimated state 1 and state 2 populations. *C*, estimation of the free phosphate (P_i) content present in WT and oncogenic mutants (Fig. 2*A*) with respect to the γ_2 population. Data are scaled to the value in WT KRAS-GTP spectra. Peak intensity error and uncertainty estimation in P_i/γ_2 peak ratio (R) were deduced using signal-to-noise ratio. The literature reported intrinsic hydrolysis rates of WT and mutant KRAS proteins (27). *D*, stack plot of spectra harboring T35S mutation.

favored in GppNHp-bound RAS, and not in GTP-bound RAS, where state 1 population is minor.

Unlike GppNHp-bound KRAS, the crystal structure of Q61H KRAS-GTP shows a highly dynamic conformation of SW2 that influences SW1 conformation resulting in more state 2-like features contributing to enhanced RAS–RAF interaction (32). Differential modulation of state 1–state 2 equilibria of GppNHp- *versus* GTP-bound HRAS (11) and KRAS (present study) is thus closely coupled with the SW dynamics that likely influences RAS–RAF interactions. This suggests revisiting GppNHp-derived protein–protein interaction data and prioritizing the use of GTP-KRAS, wherever possible, and being mindful of the impact of nonhydrolyzable nucleotide analogs on structural plasticity in RAS–effector complexes.

Interestingly, Hansen *et al.* (7) captured the lowly populated state 1 conformation in WT, G12C, and G12D KRAS-GTP using the 2D ^{1}H–^{15}N heteronuclear single quantum coherence based Carr–Purcell–Meiboom–Gill and chemical exchange saturation transfer NMR experiments. They identified state 1 and state 2 as excited state and ground state conformations, respectively (7). In agreement with our results, the major conformation of GTP-KRAS in their data belong to state 2 (90% or more population, as noted in this work). Their study demonstrates that the differentially modulated structural dynamics in WT, G12C, and G12D KRAS-GTP proteins is largely governed by the dynamics of the SW residues (7). Our NMR data argue in favor of the interpretation that SW dynamics play a critical role in regulating differential conformational plasticity in these proteins (see above). Hansen *et al.* (7) concluded that the G12C protein possesses the lowest state 1 population, an observation consistent with our results. Within the range of error values, our data show that G12C and G12D proteins likely exhibit higher state 2 population than the WT protein, in agreement with the findings reported by Hansen *et al.* (7). The G12D protein shows the slowest exchange rates for the two-state interconversion (7); our ^{31}P NMR results show the slowest intrinsic hydrolysis of G12D

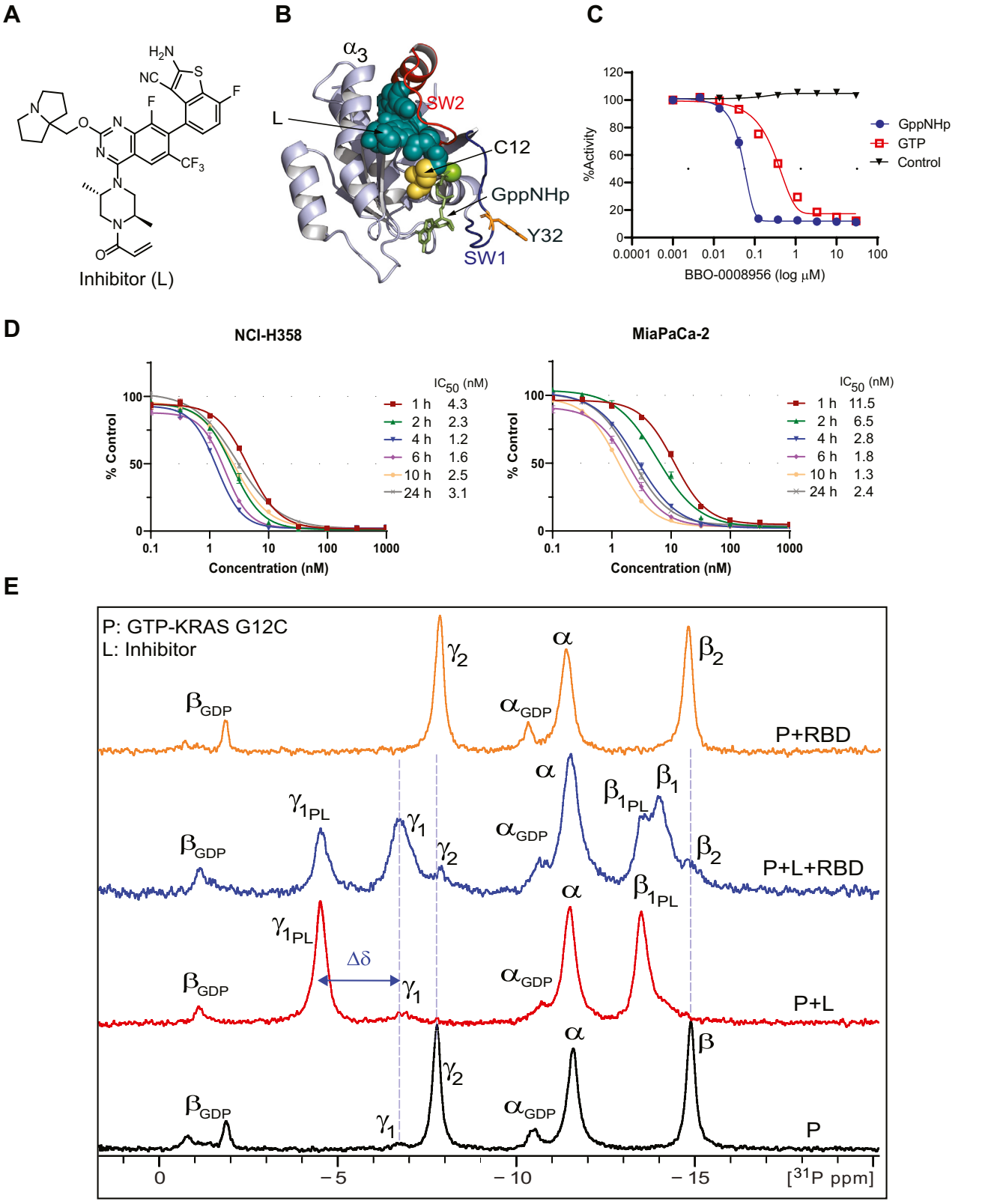

Figure 3. Identification of highly potent small-molecule inhibitor of GTP-KRAS G12C. *A*, chemical structure of novel BBO-8956 G12C inhibitor (L). *B*, *cartoon structure* shows binding site of BBO inhibitor (L) to G12C KRAS-GppNHp. *C*, disruption of KRAS G12C-RAF1 RBD binding by BBO-8956 measured by HTRF. *D*, BBO-8956 exhibits a potent and long-lasting effect on ERK phosphorylation in NCI-H358 and MiaPaCa-2 cells. IC_{50} values are average of four independent replicates. *E*, protein (P) binding of L shifts state 1–state 2 equilibrium in favor of the inactive, state 1-like conformation (induced γ_{1PL} peak located most downfield) in the protein complex (P + L) spectra. RAF1 RBD loading is unable to induce γ_2 population and establishes an equilibrium between state 1 and state 1-like conformations. Peak β_{1PL} represents L binding-induced inactive conformation of β GTP. Shown on *top* is the spectrum of P + RBD as a control. ERK, extracellular signal–regulated kinase; GppNHp, guanosine-5′-[(β,γ)-imido] triphosphate; HTRF, homogeneous time-resolved fluorescence; RBD, RAS-binding domain.

among WT, G12C, and G12D KRAS-GTP. Although we do not make a quantitative measurement of the conformational exchange rate here, we cannot rule out a link between the rates of conformational exchange and occurrence of the intrinsic hydrolysis.

Molecular dynamics simulations predict higher state 1 population for G12V KRAS-GTP

To investigate the structural rationale behind the higher state 1 population in G12V KRAS-GTP observed in NMR, we carried out a 500 ns temperature-replica exchange molecular dynamics (MD) simulation to sample the dynamics of GTP-bound KRAS WT and oncogenic mutants. The ratios of state 1 and state 2 determined from temperature-replica exchange MD simulation are listed in Fig. 2*B* (also see Fig. S3, *E*–*G*) and are similar to our NMR results. GTP-bound KRAS G12V has the highest (18%) state 1 population. Data show that χ_1 angle distributions of the codon 12 residue in C12, D12, and V12 KRAS-GTP structures sample differently (Fig. S3*G*). The χ_1 angle of V12 in KRAS-GTP exhibits evenly distributed rotamers of −60° (g+), 180° (t), and +60° (g−), whereas the dominant χ_1 rotamers in C12 and D12 are observed to occupy −60° and 180° angles, respectively. A detailed examination of state 1 or state 2 specific χ_1 distribution reveals that V12 preferentially adopts −60° rotamer in state 1 but almost evenly sampled −60°, +60°, and 180° rotamers in state 2. We hypothesize that the observance of this even distribution of these three rotamers in G12V and more specifically the enrichment of +60° rotamer provides clues to understand the elevated state 1 population in GTP-bound KRAS G12V compared with WT and other mutants of KRAS.

Effects of small-molecule KRAS GTP inhibitor on state 1–state 2 equilibrium

Covalent KRAS G12C inhibitors that advanced to the clinic bind the GDP-bound state, trapping KRAS in an inactive conformation (33, 34). Profound depletion of active KRAS-GTP that corresponds to the covalent occupancy of cysteine-12 of KRAS G12C in cells has been reported, along with inhibition of downstream RAS signaling. These reports provided evidence that KRAS G12C does cycle from GTP to GDP in cells, such that targeting its inactive GDP-bound state could sequester KRAS and exhaust the active conformation. However, only targeting the inactive conformation has been suggested to lead to resistance through increased levels of active GTP-bound KRAS driven by RTK flux or G12C amplification (35). Investigation and development of active conformation inhibitors could overcome this resistance and lead to further clinical benefit (36).

We have identified a KRAS G12C dual inhibitor (L; BBO-8956) (Fig. 3*A*) that efficiently engages the protein in both GTP and GDP conformations (Fig. S4). MALDI-TOF MS shows that the inhibitor rapidly modifies KRAS G12C-GTP, resulting in 74% and 100% covalent target modification at 5 and 30 min, respectively (Fig. S4*A*). A *cartoon structure* in Figure 3*B* shows the binding site (SIIP) of this novel G12C KRAS inhibitor. The effectiveness of this compound in disrupting KRAS G12C binding to its effector, RAF1, was assessed using a biochemical homogeneous time-resolved fluorescence assay. BBO-8956 potently disrupted KRAS G12C/RAF1(RBD) interaction with an IC_{50} of 57 nM in KRAS G12C-GppNHp and 411 nM in KRAS G12C-GTP (Fig. 3*C*). Disruption of KRAS G12C/RAF1 binding translated to a rapid and potent inhibition of mitogen-activated protein kinase signaling as evidenced by inhibition of ERK phosphorylation in KRAS G12C-mutant cell lines, lung adenocarcinoma NCI-H358 and pancreatic ductal adenocarcinoma MiaPaCa-2. Figure 3*D* shows strong and long-lasting inhibition of phosphorylated ERK signaling in both cell lines (as noted by lower IC_{50} values) observed in the BBO-8956 time-course dose response.

Using ^{31}P NMR, we have investigated the potential changes in state 1–state 2 equilibrium resulting from compound binding to SIIP pocket and covalent modification of KRAS C12 (proximal to the GTP-binding site, Fig. 3*B*). BBO-8956 binding induced a significant perturbation resulting in the emergence of highly populated γ_{1PL} peak (state 1-like; shifted by −3.3 ppm relative to γ_2) and a minimally populated γ_1 peak (Fig. 3*E*). A similar nature of perturbation is noted for β peak (shifted by −1.4 ppm relative to β_2), whereas the α peak does not show such behavior and is mostly unaffected. We confirmed the identification/assignment of γ_{1PL} peak in a separate experiment where inhibitor treatment of T35S mutant of G12C KRAS-GTP perturbed the equilibrium between the two states in a similar manner (as noted previously) in favor of "state 1-like" yielding γ_{1PL} as a major γ peak (Fig. S5), indicating that γ_{1PL} observed at −4.5 ppm represents the inactive conformation. This γ_{1PL} peak emergence is only noted in the presence of the inhibitor. The spectra of GTP-KRAS G12C alone or in the presence of RBD do not show this peak.

The chemical shifts of state 1 conformation are, generally, shifted downfield from those represented by state 2 conformation in RAS proteins ((11, 13) and internal data). This downfield shift of γ_{1PL} from γ_1 in protein–ligand complex most likely causes SW1 displacement further away from nucleotide and contributes to the enhancement of inhibitory effect that causes RAS conformation to be restricted within the inactive conformational range. These chemical shift changes occur because of the perturbed bonding pattern around γ and β P atoms as a result of the conformational changes that influence C12 and the inhibitor molecule in the P–L binary complex (Fig. 3*B*). A significant change in chemical shift of γ compared with β P atom likely indicates that the conformation of γ P is impacted more than the β P upon inhibitor binding (Fig. 3*B*). These chemical shift changes could translate to the local distances between these P atoms and juxtaposed atoms of the inhibitor and C12 site. A detailed structural analysis of this binary complex would provide more insight into these conformational arrangements.

The addition of equimolar RAF1-RBD to the G12C KRAS-GTP and BBO-8956 binary sample caused a shift of approximately half of the population from "state 1-like" to "state 1" conformation; however, no enhancement in state 2 peak

population was observed (Fig. 3*E*), suggesting the inhibitor forces the protein into an effector-binding deficient state 1 conformation (Fig. 3*B*). An excess of RBD (1:4 RAS:RAF1-RBD; a non-natural scenario of stoichiometric ratio) shifts the population from "state 1-like" to "state 1" conformation to a greater extent, while only a small fraction of the population representing state 2 conformation is noted (Fig. S5). Thus, although RAF1-RBD binds γ_1, it is not able to induce the active conformation population (γ_2) and indicates that the tricomplex (KRAS–BBO-8956–RAF1-RBD) remains locked in the (inactive) state 1 conformation (Figs. 3*B* and S5). Future studies will investigate whether RAF1-RBD indeed binds to the low-affinity binding state γ_1, or if its presence in solution just provides a rigid environment that contributes to decreasing the degree of freedom of γ_{1PL} and results in reversing the population of newly formed γ_{1PL}–γ_1 equilibrium in favor of γ_1. It has been noted that RAS mutants were nononcogenic if the presence of effectors could not convert state 1 to state 2 (11). The inability of RAF1-RBD to induce state 2 in BBO-8956–G12C KRAS–GTP complex suggests that this novel KRAS inhibitor enforces the GTP-bound protein into inactive conformation and disables effector binding.

Kalbitzer's group first demonstrated the perturbation of state 1–state 2 equilibrium of WT RAS using a metal complex inhibitor, Zn^{2+}–cyclen (a millimolar affinity binder) that binds to state 1, thereby lowering RAS affinity for RAF (37–39). A subsequent study probed the ability of compound 2 in binding to KRAS G12V state 1 (40). Binding of these ligands to GppNHp-RAS is most likely influenced by the presence of GppNHp-induced state 1. Our study investigates a novel mechanism of action (MOA) for a potent KRAS G12C inhibitor, BBO-8956, in the presence of GTP (a natural substrate). BBO-8956 induces a shift from state 2 to the inactive state 1 and through a previously unrecognized perturbation of protein dynamics. In our RAS-RAF disruption assay, BBO-8956 binding shows a lower IC_{50} in complex with GppNHp-KRAS than with GTP-KRAS. This result clearly indicates that a lower activation energy is required to convert the equilibrium state population to a state 1-like conformation in GppNHp-KRAS than in GTP-KRAS. This is due to an increased state 1 population present in GppNHp-KRAS, and likely leads to inaccurate conclusions being drawn from GppNHp-KRAS data alone when assessing the activity of the inhibitor (28).

In summary, this NMR study strengthens and extends our current understanding of state equilibrium (11) governing the biochemical properties of oncogenic KRAS and elucidates the MOA of GTP-bound KRAS G12C by a novel, direct, covalent inhibitor BBO-8956. Such an MOA approach could readily be applied to covalent and noncovalent inhibitors of KRAS as well as other GTPases.

Experimental procedures

Detailed materials and methods describing protein expression and purification, NMR sample preparation, and data acquisition and processing, MALDI-TOF MS, homogeneous time-resolved fluorescence assays for protein–protein interaction, KRAS-RBD disruption and pERK inhibition in cells, and MD simulation are provided in the supporting information. Chemical shift referencing in ^{31}P and ^{1}H NMR spectra followed a protocol as described (41). A detailed description on chemical synthesis of the compound is provided in a patent WO 2023/004102.

Data availability

All data are included within the article or supporting information.

Supporting information—This article contains supporting information (7, 11-13, 42-59).

Acknowledgments—We thank William Gillette, Matt Drew, Peter Frank, Brianna Higgins, Min Hong, Skylar Mackay, Jen Mehalko, Simon Messing, Shelley Perkins, Rosamilia Reyes, Mukul Sherekar, Kelly Snead, Troy Taylor, and Vanessa Wall for cloning, protein expression, protein purification, QC, and electrospray ionization mass spectrometry, Timothy Waybright for nucleotide loading analysis, and Drs Gabriel Cornilescu and Dhirendra Simanshu for insightful suggestions. The content of this publication does not necessarily reflect the views or policies of the Department of Health and Human Services, and the mention of trade names, commercial products, or organizations does not imply endorsement by the US Government. We thank the computing support from Lawrence Livermore National Lab (LLNL) Institutional Computing Grand Challenge program. A portion of this work was performed under the auspices of the US Department of Energy, LLNL under contract DE-AC52-07NA27344. Release: LLNL-JRNL-853388. This project was funded in part by BridgeBio Pharma, Inc under the CRADA between FNLCR and TheRas, Inc, the CRADA between LLNL and Theras, Inc (grant no.: TC02290), and with federal funds from the National Cancer Institute, National Institutes of Health contract 75N91019D00024.

Author contributions—A. K. S., F. M., and A. E. M. conceptualization; A. K. S., J. P., Y. Y., M. D., B. S., D. R., and E. K. L., methodology; A. K. S., J. P., Y. Y., M. D., B. S., D. R., and E. K. L. investigation; A. K. S., J. P., Y. Y., M. D., B. S., D. R., and E. K. L. formal analysis; M. D., F. C. L., D. E., A. G. S., B. W., P. J. B., and E. W. resources; A. K. S., D. V. N., F. M., and A. E. M. validation; A. K. S., D. V. N., F. M., and A. E. M writing–review & editing.

Funding and additional information—The content is solely the responsibility of the authors and does not necessarily represent the official views of the National Institutes of Health.

Conflict of interest—F. M. is a consultant for the following companies: Amgen; Daiichi Ltd; Frontiers Medicine; Exuma Biotech, Ideaya Biosciences; Kura Oncology; PellePharm; Pfizer, Inc; PMV Pharma; and Quanta Therapeutics. F. M. is a consultant and cofounder for the following companies (with ownership interest including stock options): BridgeBio Pharma, Inc; DNAtrix Inc; Olema Pharmaceuticals, Inc; and Quartz. F. M. is the scientific advisor of the National Cancer Institute RAS Initiative at the Frederick National Laboratory for Cancer Research/Leidos Biomedical Research, Inc. F. M. has been recipient of research grants from Daiichi Sankyo and Gilead Sciences and has a current

grant from Boehringer–Ingelheim. All the other authors declare that they have no conflicts of interest with the contents of this article.

Abbreviations—The abbreviations used are: ERK, extracellular signal–regulated kinase; GppNHp, guanosine-5′-[(β,γ)-imido] triphosphate; MD, molecular dynamics; MOA, mechanism of action; PDB, Protein Data Bank; RBD, RAS-binding domain; SW1, switch I; SW2, switch II.

References

1. Bos, J. L. (1989) Ras oncogenes in human cancer: a review. *Cancer Res.* **49**, 4682–4689
2. Downward, J. (2003) Targeting RAS signalling pathways in cancer therapy. *Nat. Rev. Cancer* **3**, 11–22
3. Hobbs, G. A., and Der, C. J. (2019) RAS mutations are not created equal. *Cancer Discov.* **9**, 696–698
4. Prior, I. A., Hood, F. E., and Hartley, J. L. (2020) The frequency of ras mutations in cancer. *Cancer Res.* **80**, 2969–2974
5. Ito, Y., Yamasaki, K., Iwahara, J., Terada, T., Kamiya, A., Shirouzu, M., *et al.* (1997) Regional polysterism in the GTP-bound form of the human c-Ha-Ras protein. *Biochemistry* **36**, 9109–9119
6. Araki, M., Shima, F., Yoshikawa, Y., Muraoka, S., Ijiri, Y., Nagahara, Y., *et al.* (2011) Solution structure of the state 1 conformer of GTP-bound H-Ras protein and distinct dynamic properties between the state 1 and state 2 conformers. *J. Biol. Chem.* **286**, 39644–39653
7. Hansen, A. L., Xiang, X., Yuan, C., Bruschweiler-Li, L., and Bruschweiler, R. (2023) Excited-state observation of active K-Ras reveals differential structural dynamics of wild-type *versus* oncogenic G12D and G12C mutants. *Nat. Struct. Mol. Biol.* **30**, 1446–1455
8. Kalbitzer, H. R., Spoerner, M., Ganser, P., Hozsa, C., and Kremer, W. (2009) Fundamental link between folding states and functional states of proteins. *J. Am. Chem. Soc.* **131**, 16714–16719
9. Spoerner, M., Wittinghofer, A., and Kalbitzer, H. R. (2004) Perturbation of the conformational equilibria in Ras by selective mutations as studied by 31P NMR spectroscopy. *FEBS Lett.* **578**, 305–310
10. Geyer, M., Schweins, T., Herrmann, C., Prisner, T., Wittinghofer, A., and Kalbitzer, H. R. (1996) Conformational transitions in p21ras and in its complexes with the effector protein Raf-RBD and the GTPase activating protein GAP. *Biochemistry* **35**, 10308–10320
11. Spoerner, M., Hozsa, C., Poetzl, J. A., Reiss, K., Ganser, P., Geyer, M., *et al.* (2010) Conformational states of human rat sarcoma (Ras) protein complexed with its natural ligand GTP and their role for effector interaction and GTP hydrolysis. *J. Biol. Chem.* **285**, 39768–39778
12. Spoerner, M., Nuehs, A., Ganser, P., Herrmann, C., Wittinghofer, A., and Kalbitzer, H. R. (2005) Conformational states of Ras complexed with the GTP analogue GppNHp or GppCH2p: implications for the interaction with effector proteins. *Biochemistry* **44**, 2225–2236
13. Spoerner, M., Herrmann, C., Vetter, I. R., Kalbitzer, H. R., and Wittinghofer, A. (2001) Dynamic properties of the Ras switch I region and its importance for binding to effectors. *Proc. Natl. Acad. Sci. U. S. A.* **98**, 4944–4949
14. Liao, J., Shima, F., Araki, M., Ye, M., Muraoka, S., Sugimoto, T., *et al.* (2008) Two conformational states of Ras GTPase exhibit differential GTP-binding kinetics. *Biochem. Biophys. Res. Commun.* **369**, 327–332
15. Johnson, C. W., Reid, D., Parker, J. A., Salter, S., Knihtila, R., Kuzmic, P., *et al.* (2017) The small GTPases K-Ras, N-Ras, and H-Ras have distinct biochemical properties determined by allosteric effects. *J. Biol. Chem.* **292**, 12981–12993
16. Parker, J. A., Volmar, A. Y., Pavlopoulos, S., and Mattos, C. (2018) K-ras populates conformational states differently from its isoform H-ras and oncogenic mutant K-RasG12D. *Structure* **26**, 810–820.e4
17. Stephen, A. G., Esposito, D., Bagni, R. K., and McCormick, F. (2014) Dragging ras back in the ring cancer. *Cell* **25**, 272–281
18. Ostrem, J. M., Peters, U., Sos, M. L., Wells, J. A., and Shokat, K. M. (2013) K-Ras(G12C) inhibitors allosterically control GTP affinity and effector interactions. *Nature* **503**, 548–551
19. Janes, M. R., Zhang, J., Li, L. S., Hansen, R., Peters, U., Guo, X., *et al.* (2018) Targeting KRAS mutant cancers with a covalent G12C-specific inhibitor. *Cell* **172**, 578–589.e7
20. Canon, J., Rex, K., Saiki, A. Y., Mohr, C., Cooke, K., Bagal, D., *et al.* (2019) The clinical KRAS(G12C) inhibitor AMG 510 drives anti-tumour immunity. *Nature* **575**, 217–223
21. Hallin, J., Engstrom, L. D., Hargis, L., Calinisan, A., Aranda, R., Briere, D. M., *et al.* (2020) The KRAS(G12C) inhibitor MRTX849 provides insight toward therapeutic susceptibility of KRAS-mutant cancers in mouse models and patients. *Cancer Discov.* **10**, 54–71
22. Weiss, A., Lorthiois, E., Barys, L., Beyer, K. S., Bomio-Confaglia, C., Burks, H., *et al.* (2022) Discovery, preclinical characterization, and early clinical activity of JDQ443, a structurally novel, potent, and selective covalent oral inhibitor of KRASG12C. *Cancer Discov.* **12**, 1500–1517
23. Schulze, C. J., Seamon, K. J., Zhao, Y., Yang, Y. C., Cregg, J., Kim, D., *et al.* (2023) Chemical remodeling of a cellular chaperone to target the active state of mutant KRAS. *Science* **18**, 794–799
24. Muraoka, S., Shima, F., Araki, M., Inoue, T., Yoshimoto, A., Ijiri, Y., *et al.* (2012) Crystal structures of the state 1 conformations of the GTP-bound H-Ras protein and its oncogenic G12V and Q61L mutants. *FEBS Lett.* **586**, 1715–1718
25. Ingolfsson, H. I., Neale, C., Carpenter, T. S., Shrestha, R., Lopez, C. A., Tran, T. H., *et al.* (2022) Machine learning-driven multiscale modeling reveals lipid-dependent dynamics of RAS signaling proteins. *Proc. Natl. Acad. Sci. U. S. A.* **119**, e2113297119
26. Chao, F. A., Chan, A. H., Dharmaiah, S., Schwieters, C. D., Tran, T. H., Taylor, T., *et al.* (2023) Reduced dynamic complexity allows structure elucidation of an excited state of KRAS(G13D). *Commun. Biol.* **6**, 594
27. Hunter, J. C., Manandhar, A., Carrasco, M. A., Gurbani, D., Gondi, S., and Westover, K. D. (2015) Biochemical and structural analysis of common cancer-associated KRAS mutations. *Mol. Cancer Res.* **13**, 1325–1335
28. Long, D., Marshall, C. B., Bouvignies, G., Mazhab-Jafari, M. T., Smith, M. J., Ikura, M., *et al.* (2013) A comparative CEST NMR study of slow conformational dynamics of small GTPases complexed with GTP and GTP analogues. *Angew. Chem. .Int. Ed. Engl.* **52**, 10771–10774
29. Moghadamchargari, Z., Huddleston, J., Shirzadeh, M., Zheng, X., Clemmer, D. E., Raushel, F. M., *et al.* (2019) Intrinsic GTPase activity of K-RAS monitored by native mass spectrometry. *Biochemistry* **58**, 3396–3405
30. Johnson, C. W., Lin, Y. J., Reid, D., Parker, J., Pavlopoulos, S., Dischinger, P., *et al.* (2019) Isoform-specific destabilization of the active site reveals a molecular mechanism of intrinsic activation of KRas G13D. *Cell Rep.* **28**, 1538–1550.e7
31. Pantsar, T. (2020) The current understanding of KRAS protein structure and dynamics. *Comput. Struct. Biotechnol. J.* **18**, 189–198
32. Zhou, Z. W., Ambrogio, C., Bera, A. K., Li, Q., Li, X. X., Li, L., *et al.* (2020) KRAS(Q61H) preferentially signals through MAPK in a RAF dimer-dependent manner in non-small cell lung cancer. *Cancer Res.* **80**, 3719–3731
33. Lito, P., Solomon, M., Li, L. S., Hansen, R., and Rosen, N. (2016) Allele-specific inhibitors inactivate mutant KRAS G12C by a trapping mechanism. *Science* **351**, 604–608
34. Patricelli, M. P., Janes, M. R., Li, L. S., Hansen, R., Peters, U., Kessler, L. V., *et al.* (2016) Selective inhibition of oncogenic KRAS output with small molecules targeting the inactive state. *Cancer Discov.* **6**, 316–329
35. Awad, M. M., Liu, S., Rybkin, I. I., Arbour, K. C., Dilly, J., Zhu, V. W., *et al.* (2021) Acquired resistance to KRAS(G12C) inhibition in cancer. *N. Engl. J. Med.* **384**, 2382–2393
36. Tanaka, N., Lin, J. J., Li, C., Ryan, M. B., Zhang, J., Kiedrowski, L. A., *et al.* (2021) Clinical acquired resistance to KRAS(G12C) inhibition through a novel KRAS switch-II pocket mutation and polyclonal alterations converging on RAS-MAPK reactivation. *Cancer Discov.* **11**, 1913–1922
37. Spoerner, M., Graf, T., Konig, B., and Kalbitzer, H. R. (2005) A novel mechanism for the modulation of the Ras-effector interaction by small molecules. *Biochem. Biophys. Res. Commun.* **334**, 709–713

38. Rosnizeck, I. C., Filchtinski, D., Lopes, R. P., Kieninger, B., Herrmann, C., Kalbitzer, H. R., *et al.* (2014) Elucidating the mode of action of a typical Ras state 1(T) inhibitor. *Biochem* **53**, 3867–3878
39. Rosnizeck, I. C., Spoerner, M., Harsch, T., Kreitner, S., Filchtinski, D., Herrmann, C., *et al.* (2012) Metal-bis(2-picolyl)amine complexes as state 1(T) inhibitors of activated Ras protein. *Angew. Chem. Int. Ed. Engl.* **51**, 10647–10651
40. Jansen, J. M., Wartchow, C., Jahnke, W., Fong, S., Tsang, T., Pfister, K., *et al.* (2017) Inhibition of prenylated KRAS in a lipid environment. *PLoS One* **12**, e0174706
41. Maurer, T., and Kalbitzer, H. R. (1996) Indirect referencing of 31P and 19F NMR spectra. *J. Magn. Reson. B* **113**, 177–178
42. Esposito, D., Garvey, L. A., and Chakiath, C. S. (2009) Gateway cloning for protein expression. *Methods Mol. Biol.* **498**, 31–54
43. Wall, V. E., Garvey, L. A., Mehalko, J. L., Procter, L. V., and Esposito, D. (2014) Combinatorial assembly of clone libraries using site-specific recombination. *Methods Mol. Biol.* **1116**, 193–208
44. Taylor, T., Denson, J. P., and Esposito, D. (2017) Optimizing expression and solubility of proteins in E. coli using modified media and induction parameters. *Methods Mol. Biol.* **1586**, 65–82
45. Kopra, K., Vuorinen, E., Abreu-Blanco, M., Wang, Q., Eskonen, V., Gillette, W., *et al.* (2020) Homogeneous dual-parametric-coupled assay for simultaneous nucleotide exchange and KRAS/RAF-RBD interaction monitoring. *Anal. Chem.* **92**, 4971–4979
46. Sharma, A. K., Dyba, M., Tonelli, M., Smith, B., Gillette, W. K., Esposito, D., *et al.* (2022) NMR (1)H, (13)C, (15)N backbone resonance assignments of the T35S and oncogenic T35S/Q61L mutants of human KRAS4b in the active, GppNHp-bound conformation. *Biomol. NMR Assign.* **16**, 1–8
47. Case, D. A., Aktulga, H. M., Belfon, K., Ben-Shalom, I. Y., Berryman, J. T., Brozell, S. R., *et al.* (2023) *Amber 2023*. University of California, San Francisco, San Francisco, CA
48. Sugita, Y., and Okamoto, Y. (1999) Replica-exchange molecular dynamics method for protein folding. *Chem. Phys. Lett.* **314**, 141–151
49. Maier, J. A., Martinez, C., Kasavajhala, K., Wickstrom, L., Hauser, K. E., and Simmerling, C. (2015) ff14SB: improving the accuracy of protein side chain and backbone parameters from ff99SB. *J. Chem. Theory Comput.* **11**, 3696–3713
50. Meagher, K. L., Redman, L. T., and Carlson, H. A. (2003) Development of polyphosphate parameters for use with the AMBER force field. *J. Comput. Chem.* **24**, 1016–1025
51. Ryckaert, J.-P., Cicotti, G., and Berendsen, H. J. C. (1977) Numerical-integration of Cartesian equations of motion of a system with constraints - molecular-dynamics of N-Alkanes. *J. Comput. Phys.* **23**, 327–341
52. Darden, T., Darrin, Y., and Pedersen, L. (1993) Particle Mesh Ewald - an N.Log(N) method for Ewald sums in large systems. *J. Chem. Phys.* **98**, 10089–10092
53. Essmann, U., Perera, L., Berkowitz, M. L., Darden, T., Lee, H., and Pedersen, L. G. (1995) A smooth Particle Mesh Ewald method. *J. Chem. Phys.* **103**, 8577–8593
54. Tran, T. H., Chan, A. H., Young, L. C., Bindu, L., Neale, C., Messing, S., *et al.* (2021) KRAS interaction with RAF1 RAS-binding domain and cysteine-rich domain provides insights into RAS-mediated RAF activation. *Nat. Commun.* **12**, 1176
55. Fetics, S. K., Guterres, H., Kearney, B. M., Buhrman, G., Ma, B., Nussinov, R., *et al.* (2015) Allosteric effects of the oncogenic RasQ61L mutant on Raf-RBD. *Structure* **23**, 505–516
56. Pacold, M. E., Suire, S., Perisic, O., Lara-Gonzalez, S., Davis, C. T., Walker, E. H., *et al.* (2000) Crystal structure and functional analysis of Ras binding to its effector phosphoinositide 3-kinase gamma. *Cell* **103**, 931–943
57. Kalbitzer, H. R., Spoerner, M., Ganser, P., Hozsa, C., and Kremer, W. (2009) Fundamental link between folding states and functional states of proteins. *J. Am. Chem. Soc.* **131**, 16714–16719
58. Menyhard, D. K., Palfy, G., Orgovan, Z., Vida, I., Keseru, G. M., and Perczel, A. (2020) Structural impact of GTP binding on downstream KRAS signaling. *Chem. Sci.* **11**, 9272–9289
59. Sharma, A. K., Lee, S.-J., Zhou, M., Rigby, A. C., and Townson, S. A. (2019) NMR ^{1}H,^{13}C, ^{15}N resonance assignment of the G12C mutant of human K-Ras bound to GppNHp. *Biomol. NMR Assign.* **13**, 227–231